Pharm Res (2013) 30:523–537
DOI 10.1007/s11095-012-0898-y

RESEARCH PAPER

Evaluation of Wound Healing Potential of β-Chitin Hydrogel/Nano Zinc Oxide Composite Bandage

Sudheesh Kumar P. T. • Vinoth-Kumar Lakshmanan • Mincy Raj • Raja Biswas • Tamura Hiroshi • Shantikumar V. Nair • Rangasamy Jayakumar

Received: 9 July 2012 / Accepted: 8 October 2012 / Published online: 8 November 2012

ABSTRACT

Purpose β-chitin hydrogel/nZnO composite bandage was fabricated and evaluated in detail as an alternative to existing bandages.

Methods β-chitin hydrogel was synthesized by dissolving β-chitin powder in Methanol/$CaCl_2$ solvent, followed by the addition of distilled water. ZnO nanoparticles were added to the β-chitin hydrogel and stirred for homogenized distribution. The resultant slurry was frozen at 0°C for 12 h. The frozen samples were lyophilized for 24 h to obtain porous composite bandages.

Results The bandages showed controlled swelling and degradation. The composite bandages showed blood clotting ability as well as platelet activation, which was higher when compared to the control. The antibacterial activity of the bandages were proven against *Staphylococcus aureus (S. aureus)* and *Escherichia coli (E.coli)*. Cytocompatibility of the composite bandages were assessed using human dermal fibroblast cells (HDF) and these cells on the composite bandages were viable similar to the Kaltostat control bandages and bare β-chitin hydrogel based bandages. The viability was reduced to 50–60% in bandages with higher concentration of zinc oxide nanoparticles (nZnO) and showed 80–90% viability with lower concentration of nZnO. *In vivo* evaluation in Sprague Dawley rats (S.D. rats) showed faster healing and higher collagen deposition ability of composite bandages when compared to the control.

Conclusions The prepared bandages can be used on various types of infected wounds with large volume of exudates.

S. P. T. • V.-K. Lakshmanan • M. Raj • R. Biswas • S. V. Nair • R. Jayakumar (✉)
Amrita Centre for Nanosciences and Molecular Medicine
Amrita Institute of Medical Sciences and Research Centre
Amrita Vishwa Vidyapeetham University
Kochi 682041, India
e-mail: rjayakumar@aims.amrita.edu; jayakumar77@yahoo.com

T. Hiroshi
Faculty of Chemistry, Materials and Bioengineering, Kansai University
Osaka 564-8680, Japan

KEY WORDS antibacterial · bandage · nano ZnO · wound healing · β-chitin hydrogel

INTRODUCTION

Wound is a type of injury occurring due to various reasons like surgery, trauma, burn, diabetes, etc. Among these, burn and diabetic foot ulcers are becoming life threatening problems (1). According to reports, ~10 million people are suffering from burn and chronic wounds worldwide (1). These types of wounds require proper treatment at the right time. Use of ideal wound dressing material possessing adequate features can aid in better wound healing and patient comfort. The features of an ideal wound dressing is that it should possess adequate mechanical strength, flexibility, tear resistance and should not adhere onto the wounds (2). It should be capable of absorbing large volume of wound exudates from the wound surface, especially in burn, chronic and diabetic wounds where the volume of exudate is usually high (3). It should act as a barrier against microbes and should prevent the growth of micro-organisms on the wound surface (4). It should be porous in nature so that it can allow the gaseous exchange in and out of the wound surface (3). Ideally, it would be good if a wound dressing material is biodegradable so that peeling off the material can be avoided where it is necessary to be retained.

Various types of materials are available commercially for the treatment of wounds (5). These materials include powder, ointment, cream, gel, spray, gauze and bandages. All these materials are made either from natural materials like alginate, hyaluronic acid, collagen, gelatin, chitin, chitosan etc. or from synthetic materials like poly(lactic acid), poly(L-lactic-co-glycolic acid), poly(urethane), poly(3-hydroxybutyrate-co-3-hydroxyvalerate), poly(ethyleneimine) etc. (5–12). These materials are having advantages as well as disadvantages. Majority of these materials have shown good impact on normal wound healing but its effect on a chronic or diabetic foot

ulcer is yet to be studied (6,7). Most of these materials do not possess adequate mechanical strength and flexibility (8). Some of these materials do not have blood clotting ability whereas some lacked antibacterial activity (9). Another problem with these materials is its non-biodegradable nature and majority of these materials are costly as well. Considering all these factors, it is important to develop a new wound dressing material which possesses all the essential requirements of an ideal wound dressing material.

Chitin is a polysaccharide which is the most abundant natural polymer on earth after cellulose and the main sources of chitin are crabs, shrimps, lobsters etc. (10). Chitin possesses different polymorphic forms such as α, β and γ (13). Based on the arrangement of polymer chains, their properties will also vary. Chitin and its major derivative chitosan are being introduced into the wound dressing area by many researchers (4,7,11,14,15). These materials are biodegradable, hemostatic, cytocompatible and can easily be converted into many forms like hydrogel, bead, fiber, membrane etc. (13,16–23). β-chitin is gaining more attention in the wound dressing field as well as for other biomedical applications (24–27). The sources of β-chitin are squid pen, pens of loligo etc. (28,29). In our previous study we have reported the use of scaffolds for wound dressings made from β-chitin hydrogel (24). Many others have also reported the use of this material in this field (24,30,31). Their drawbacks include lack of mechanical strength, poor blood clotting ability and reduced swelling ability (23,31).

In vitro genotoxic effect of ZnO nanoparticles on human keratinocytes, neural cells, epidermal cells has been reported (32–34). Certain studies have proved that concentrations as low as 0.2ug/ml have DNA damaging effects on squamous cell carcinoma (35). Nair *et al.* reported that, nZnO possesses potent antibacterial activity but has no adverse effect on normal cells at appropriate concentrations (36). These *in vitro* toxic concentrations may have contradictory *in vivo* results (37,38). Detailed *in vivo* investigations of these nanoparticles are needed to get an idea of their toxicological impact under *in vivo* conditions. Hence it is important to perform *in vivo* studies in animal models.

In this work, we are focusing on the development and extensive evaluation of micro-porous and flexible bandages from β-chitin hydrogel. We are also evaluating the role of ZnO nanoparticles for both antibacterial and antifungal activity and thereby its role in wound healing (39).

MATERIALS AND METHODS

Materials

β-chitin (Molecular Weight 150 KDa, Degree of Acetylation-72.4%) was purchased from Koyo chemical Co Ltd, Japan. *β*-chitin was isolated from squid pen. Sodium hydroxide and hen egg lysozyme were purchased from Qualigens chemicals, India. *S. aureus* (ATCC 25923) and *E.coli* (ATCC 25922) strains were provided by Microbiology lab of Amrita Institute of Medical Sciences, Kochi, India. DAPI (4′,6-diamidino-2-phenylindole) was purchased from Invitrogen. Phalloidin dye was purchased from Sigma-Aldrich. Human dermal fibroblast cells (HDF) and growth medium were purchased from Promocell, Germany. Luria-Bertani broth (L.B broth), Agar-Agar, and Sabouraud Chloramphenicol Agar (S.C agar) were purchased from Himedia, India. All chemicals were used without further purification.

Synthesis of β-Chitin Hydrogel/nZnO Composite Bandage

β-chitin hydrogel was prepared according to our previously reported method. In brief, β-chitin powder was dissolved in Methanol/$CaCl_2$ solvent, followed by the addition of distilled water which resulted in the hydrogel formation. The obtained hydrogel was purified by dialysis (24). nZnO was prepared by adding NaOH solution to Zinc acetate solution at 60°C under stirring. The obtained nZnO was then purified by centrifugation (39). Composite bandage preparation was done as follows. Stable suspension of nZnO was prepared by suspending nZnO in water followed by probe sonication for 15 min by providing sonication energy of 45,800 J. The prepared nano suspension was added drop wise to β-chitin hydrogel under vigorous stirring and kept for 1 h without disturbance. The uniform mixture of nZnO and β-chitin hydrogel was then transferred to Teflon moulds and freeze-dried. The prepared composite bandages were used for further studies.

Characterization

The porous structure and surface nature of β-chitin hydrogel/nZnO composite bandages were characterized by scanning electron microscope (JEOL, JSM-6490LA, Japan). β-chitin hydrogel/nZnO composite bandages were characterized using FT-IR (PerkinElmer Co, SPECTRUM RX1, FT-IR) and X-Ray diffraction (PANalytical X'Pert PRO, Cu Kα radiation, operating at a voltage of 40 kV).

Porosity of β-Chitin Hydrogel/nZnO Composite Bandage

Porosity of the composite bandages were evaluated by alcohol displacement method (39). Briefly, small pieces of pre-weighed bandages were immersed in alcohol. After 24 h the bandage pieces were taken out and the

final weight was noted. Porosity was calculated by the following formula

$$P = (W_2 - W_1)/(\rho V_1)$$

Where W_1 and W_2 indicates the weight of the bandages before and after immersing, respectively, and V_1 is the volume before immersing, ρ is a constant of the density of alcohol. Experiment was done thrice and the average values were taken.

Swelling Ratio of β-Chitin Hydrogel/nZnO Composite Bandage

Bandage pieces of similar size and weight were immersed in Phosphate Buffered saline (PBS) having pH 7.4 at 37°C. The bandage pieces were taken out at different time intervals and swollen weight was noted. Swelling ratio was calculated using the formula given below

$$DS = [(W_w - W_d)/W_d] \times 100$$

In Vitro Biodegradation of β-Chitin Hydrogel/nZnO Composite Bandage

This was done based on the reported method (39). Briefly, bandages were evenly weighed and immersed in lysozyme (10,000 U/mL) containing medium and incubated at 37°C for 21 days. Original weight of the bandage was noted as W_i. After 7, 14 and 21 days, each set of bandages were taken out from the PBS containing lysozyme,washed with deionised water to get rid of the ions adsorbed on the surface followed by freeze-drying. The dry weight was noted as W_t. The rate of degradation of bandage was calculated using the formula

$$\text{Degradation}(\%) = (W_i - W_t)/W_i \times 100$$

Release Study of nZnO by Inductively Coupled Plasma-Optical Emission Spectrometry (ICP-OES)

The quantity of nZnO contained and released from the bandage was done by ICP-OES (Perkin Elmer Optima 5300DV). The quantification of nZnO contained in the bandage was determined as follows. Bandage pieces with 2 cm^2 area and 50 mg weight were treated with Conc. HNO_3− Conc. $HClO_4$ mixture in a microwave digestion system (Multiwave 3000, Anton Paar). Win Lab 32 software was used to record and analyze the data. For nZnO release study, bandage pieces were immersed in PBS having pH 7.4 at 37°C. The release of nZnO immediately and after 1 week of immersion in PBS was analyzed by ICP-OES.

Evaluation of Mechanical Properties of β-Chitin Hydrogel/nZnO Composite Bandage

Tensile strength was measured as follows; the bandage pieces were cut in the dimension of 10×2×0.4 cm. The ends of bandages were clipped with a special gripper. The tensile strength and percentage of elongation at the point of breakage of the bandages were measured by a universal testing machine (Instron 3365) with a load cell of 5 kN and the crosshead speed was 25 $mm\,min^{-1}$ at room temperature. Both elongation at break and tensile strength were noted. Kaltostat™ was taken as the positive control.

Haemostatic Potential of β-Chitin Hydrogel/nZnO Composite Bandage

Haemostatic potential of the bandages were assessed by doing the blood clotting analysis and platelet activation (4). Blood clotting study was conducted as follows; human blood was collected from the ulnar vein using sterile syringe and mixed with anticoagulant citrate dextrose (ACD). 100 µl ACD-Blood mixture was poured on the bandages and 5 µl of 0.2 M $CaCl_2$ was added to this to initiate the clotting. This was incubated at 37°C for 20 min with shaking. Blood clotting was analyzed by measuring the optical density at 540 nm using a plate reader (BioTek PowerWave XS).

In Vitro Antibacterial and Antifungal Activity Evaluation

The antibacterial activity was evaluated against gram positive *S. aureus* and gram negative *E. coli*. The antifungal activity was evaluated against *Candida albicans*. The strains were cultured in L.B. broth and transferred to fresh and sterile plastic tubes containing L.B. broth to get a concentration of 1×10^6 Colony forming unit (CFU)/ml (39). The bandage pieces which were pre-sterilized were added to the tubes and kept for incubation at 37°C for 24 h. After the specified time period, L.B. broth containing the bacteria and fungus were serially diluted in sterile saline and plated on L.B. and S.C. agar plates respectively. The number of bacterial colonies were counted and plotted to quantify the antibacterial activity.

Cell Viability Evaluation

Cell viability was measured by Alamar blue assay (39). In brief, the bandage pieces were sterilized by ethylene oxide gas (ETO) and were placed in well plates. HDF cells were cultured in 25 cm^2 culture flasks. Cells were trypsinized after reaching a confluency of 80% and seeded at a density of 5,000 cells/bandage piece and immersed in cell culture medium in 12 well plate. The samples were kept for incubation up to 72 h. After 24, 48 and 72 h the culture medium was removed and medium

with alamar blue was added to the wells and again kept for incubation for 4–6 h. After the incubation period the viability was measured by reading the optical density at 570 nm with 620 nm as the reference wavelength using a microplate spectrophotometer (Biotek Power Wave XS, USA).

Cell Attachment and DAPI Staining

HDF cells were seeded on the bandages at a density of 10,000 cells and kept for 24 h of incubation. After incubation, the bandages were washed with PBS and fixed with 1% glutaraldehyde solution for 1 h. The samples were thoroughly washed with PBS and dehydrated in a graded ethanol series, air-dried, gold sputtered in vacuum and examined with SEM.

DAPI or 4′, 6-diamidino-2-phenylindole was used as nuclear stain. The cell seeded bandages were fixed with 4% paraformaldehyde for 20 min, permeabilised with 0.5% Triton X-100 (in PBS) for 5 min. Then the bandages were treated with 1% FBS, washed with PBS and stained with 50 µL of DAPI and incubated in dark for 3 min. The bandages were then washed with PBS and viewed under fluorescent microscope (Olympus-BX-51). The bandages with seeded cells (48 h) were treated with TRITC conjugated Phalloidin dye and images were taken using confocal microscope (Leica SP 5 II).

Cell Infiltration Analysis of β-Chitin Hydrogel/nZnO Composite Bandage

HDF cells were seeded at a density of 10,000 cells onto the bandage pieces and cultured for 48 h. After incubation, the culture medium was discarded and the bandage pieces were washed with PBS. The cells were fixed with 4% paraformaldehyde for 15 min and washed with PBS. The cell permeabilization and blocking steps were carried out using 0.5% triton for 10 min and 1% bovine serum albumin for 20 min respectively. The samples were incubated in dark with TRITC conjugated phalloidin for 1 h. Images were taken by laser confocal microscope.

In Vivo Evaluation in Sprague–Dawley Rats

In vivo animal study was done after getting the approval from Institutional Animal Ethical Committee (IAEC), Amrita Institute of Medical Sciences and Research Center, Cochin, India. Sprague–Dawley (SD) rats weighing 200–250 g and 4–6 weeks age were used in this study. The rats were randomly divided into 5 groups and each group contained 6 rats (n=6). Rats were allowed to take normal rat feed and water without restriction. On the day of surgery; the rats were anaesthetized by intramuscular injection of 35.0 mg/kg Ketamine and 5.0 mg/kg Xylazine. The dorsal area of the rats was depilated and the operative area of the skin was cleaned with alcohol. Partial thickness skin wound of size 1.5 cm^2 was prepared by excising the dorsum of the rat using surgical scissors and forceps. The β-chitin hydrogel/nZnO composite bandages, β-chitin hydrogel control bandage and Kaltostat were then applied on the wounds. Rats with bare wound were kept as negative control. After experimental procedure rats were individually housed under normal room temperature. Dressing materials were removed after each week to observe and measure the wound closure. Wound area closure was measured by marking the area on a transparent sheet by placing the transparent sheet on the wound surface. The area on the sheet was transferred to a graph sheet to measure the exact area. New dressings were applied after measuring the area and again housed in individual cages.

Hematoxylin-Eosin and Picro-Sirius Red Staining

Skin wound tissue was excised after 1 and 3 weeks and fixed with 10% formalin solution. The tissues were processed in different grades of alcohol and xylene. Tissues were then embedded in paraffin wax and 5 µm thick sections were taken. Tissue sections were stained with Harris's Hematoxylin-Eosin (H&E) reagent for histological observations under light microscopy.

Tissue sections were stained with Picro-Sirius red for collagen staining as well as for quantification of collagen content on the healed wound area. Quantification of collagen content was done by histomorphometry using the Image Pro software, USA. Histomorphometry is a software assisted analysis of images taken by a microscope from the tissue sections in which the quantitative study of the tissues and structure of a tissue can be evaluated.

In Vivo Antibacterial Activity Evaluation

In vivo antibacterial efficacy of the bandage was assessed by taking swabs from the rat wound after 1st and 2nd week of the experiments and cultured in L.B. broth. After incubation, bacteria were streaked on L.B. agar plates and the shape of bacteria was noted and found them to be rod and round shaped bacteria. The bacteria were again cultured on L.B. agar plates separately based on their shapes and identification of the same was done by biochemical assay. Biochemical assay consists of gram staining, coagulase, catalase, oxidase and DNase tests. The bacteria isolated from the rat wound were quantified as follows. The bacteria were cultured in L.B.broth and then serially diluted in normal saline and plated on L.B. Agar plates. The number of bacterial colonies were counted and plotted for quantification.

Statistics Analysis

The data presented in this study was obtained by taking the average of three independent experiments with triplicates. The values were expressed as means±standard deviation (SD).

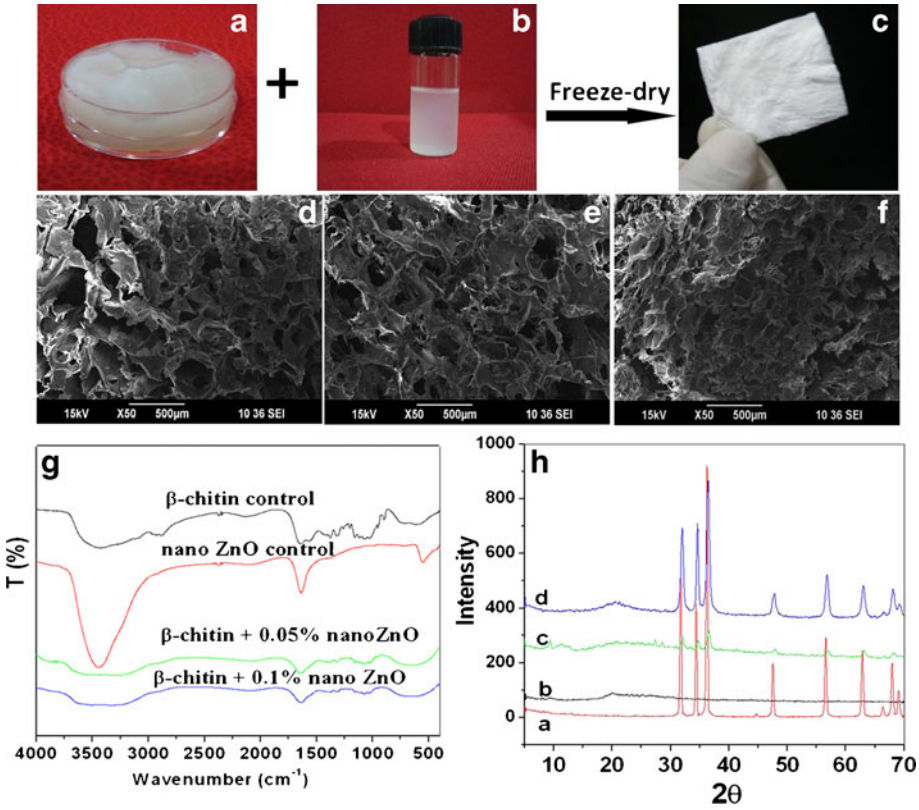

Fig. 1 Photographs of (**a**) β-chitin hydrogel, (**b**) nZnO suspension, (**c**) β-chitin hydrogel/nZnO composite bandage. SEM images of (**d**) β-chitin control, (**e**) β-chitin + 0.1% nZnO and (**f**) β-chitin + 0.05% nZnO. (**g**) FT-IR spectra of composite bandages. (**h**) XRD spectra of (*a*) nZnO control (*b*) β-chitin control (*c*) β-chitin + 0.05% nZnO and (*d*) β-chitin + 0.1% nZnO.

Statistical significance was checked by performing student's *t* test and the data with p value <0.05 was considered significant.

RESULTS

Characterization

Figure 1 a, b, c represents the photographs of β-chitin hydrogel, nZnO suspension and composite bandage respectively. SEM images of composite bandages (Fig. 1d, e, f) proved that the addition of nZnO slightly affected the surface morphology. This was due to the interaction of nZnO with β-chitin. The pore size of the bandage was in the range of 200–400 μm and showed an interconnected porous structure. The presence of nZnO in the composite bandages was confirmed by FT-IR (Fig. 1g) and XRD (Fig. 1h). Figure 1g shows the FT-IR spectra of β-chitin hydrogel/nZnO composite bandages. The spectrum of β-chitin showed a characteristic peak at 1,654 cm^{-1} which corresponds to the primary amide groups of β-chitin.

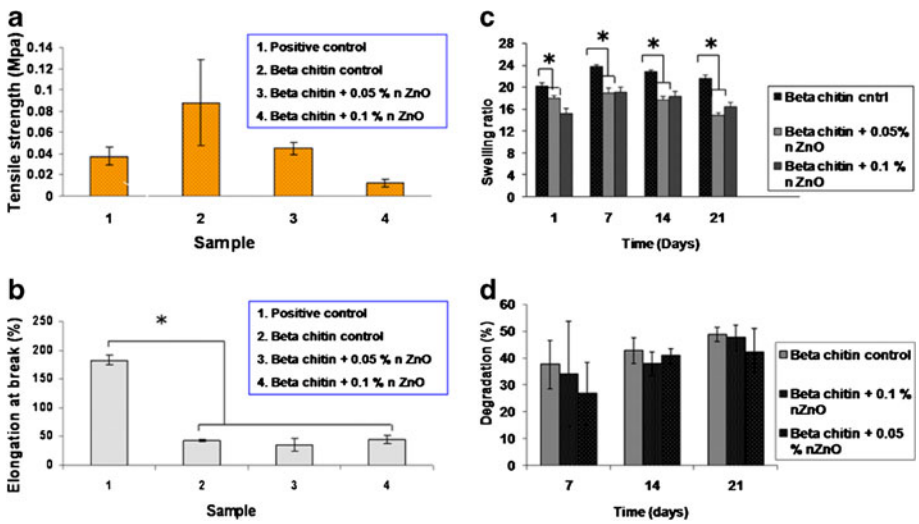

Fig. 2 (**a**) Tensile strength of composite bandages. (**b**) Elongation at break of composite bandages. (**c**) Swelling ratio evaluation of composite bandages in PBS. (**d**) Biodegradation evaluation of the composite bandages.

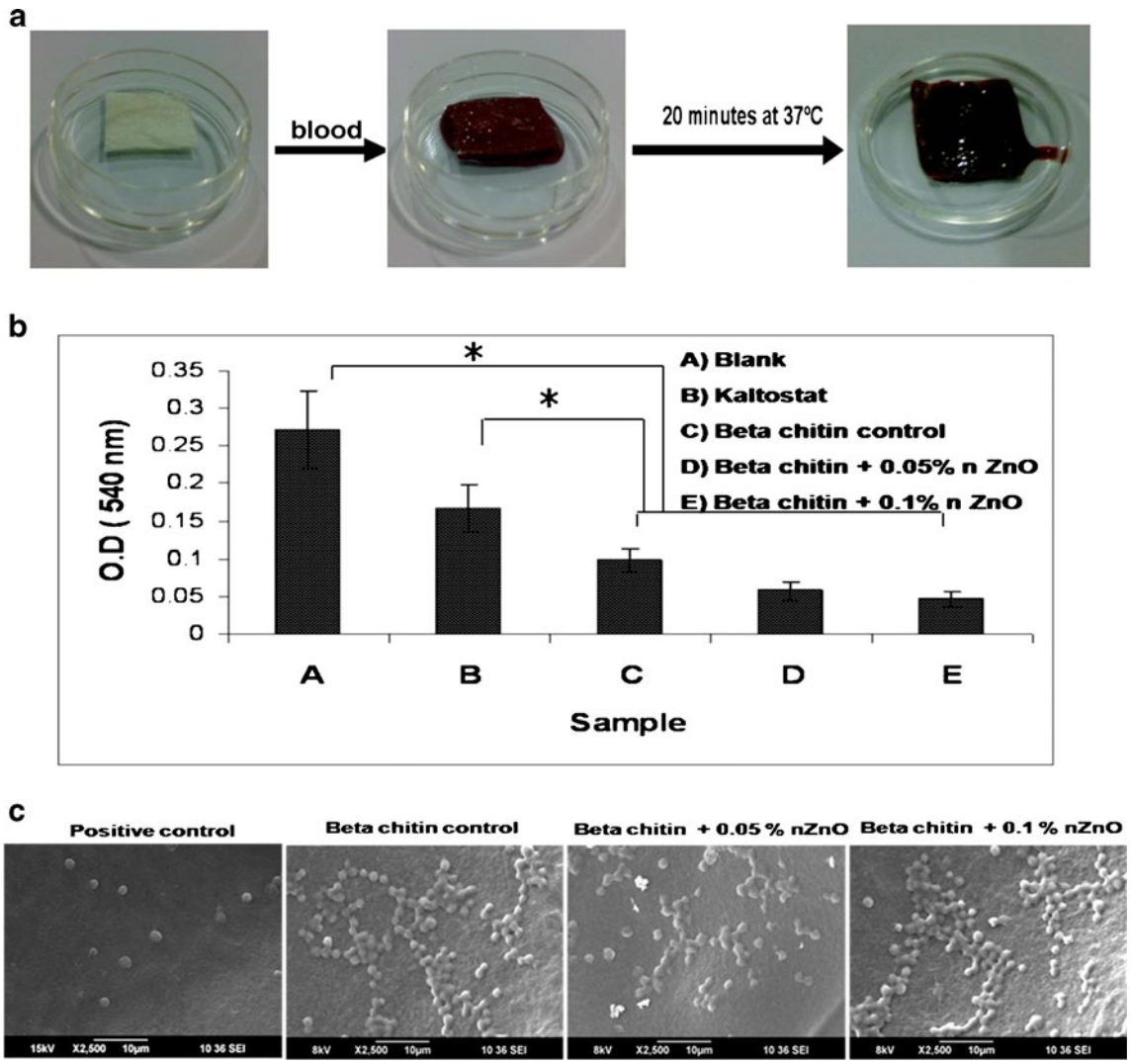

Fig. 3 (**a**) Photographs of composite bandage, blood on bandage and bandage with blood clot. (**b**) Blood clotting evaluation of composite bandages. (**c**) SEM images of platelets attached on the banadages.

The peak at 1,070 cm^{-1} corresponds to glycosidic linkage whereas the peak at 3,450 cm^{-1} corresponds to the hydroxyl group. Spectra of nZnO showed characteristic peak of ZnO at 510 cm^{-1} (24,39,40). Figure 1h represents the XRD spectra of β-chitin hydrogel/nZnO composite bandages. XRD spectra showed the characteristic peak of β-chitin control at 20.5°. The characteristic peaks of nZnO peaks at 31.6, 34.3, 36.2, 56.5, 62.8 and 67.8° (JCPDS file no. 89–1397) were present in the spectra of composite bandages along with peaks of β-chitin (39,40).

Mechanical Properties of β-Chitin Hydrogel/nZnO Composite Bandage

The bandages showed tensile strength in the range of 0.02 MPa to 0.05 MPa except the bandage with higher concentration of nZnO (0.1%) which showed tensile strength of 0.02 MPa. The decrease in tensile strength was due to the interaction of nZnO with the chitin matrix (Fig. 2a). All the bandages except positive control showed 50% elongation at break (Fig. 2b) and it indicate the bandages were highly flexible and can be used to apply wounds where flexibility demands most.

Porosity, Swelling Ratio and Biodegradation of β-Chitin Hydrogel/nZnO Composite Bandage

Porosity was determined by alcohol displacement method. β-chitin control bandages showed porosity of ~70–80% of the total bandage volume whereas nZnO incorporated composite bandages showed porosity of ~60–70%. The minor reduction in the porosity was due to the interaction of β-chitin with nZnO.

Swelling ratio of the bandages was evaluated (Fig. 2c) and the control bandages showed a swelling ratio of 20. The presence of nZnO slightly reduced the swelling

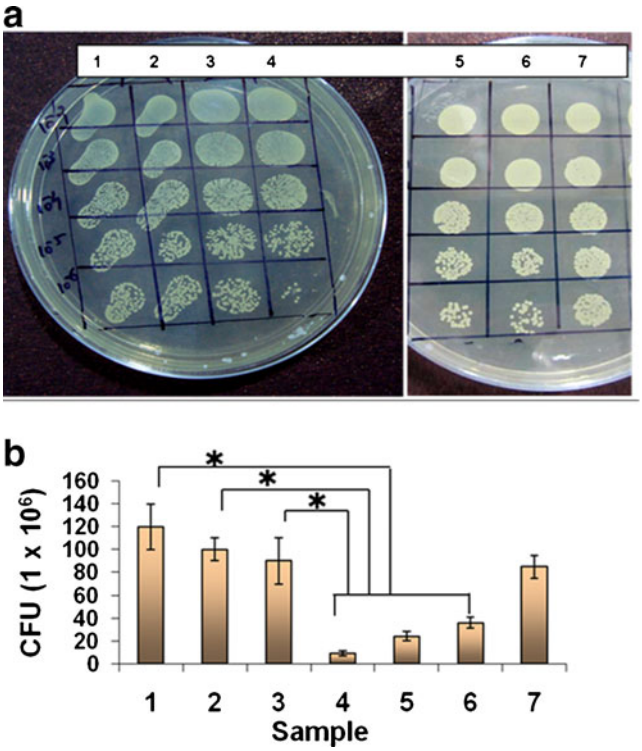

Fig. 4 (**a**) Photographs of antibacterial activity and (**b**) quantification of antibacterial activity against *S. aureus* (*1*) *S. aureus* control (*2*) Kaltostat (*3*) β-chitin control (*4*) β-chitin + 0.1% nZnO (*5*) β-chitin + 0.05% nZnO (*6*) β-chitin + 0.025% nZnO (*7*) β-chitin + 0.01% nZnO.

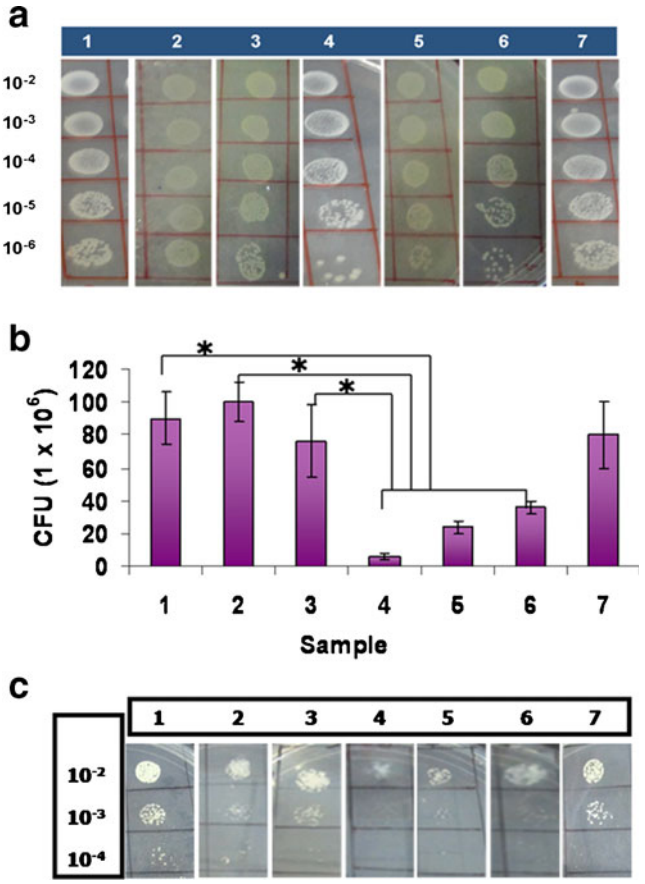

Fig. 5 (**a**) Photographs and (**b**) quantification data of antibacterial activity studies against *E. coli* (*1*) *E. coli* control (*2*) Kaltostat (*3*) β-chitin control (*4*) β-chitin + 0.1% nZnO (*5*) β-chitin + 0.05% nZnO (*6*) β-chitin + 0.025% nZnO (*7*) β-chitin + 0.01% nZnO. (**c**) Antifungal study against *Candida albicans* (*1*) *Candida albicans* control (*2*) Kaltostat (*3*) β-chitin control (*4*) β-chitin + 0.1% nZnO (*5*) β-chitin + 0.05% nZnO (*6*) β-chitin + 0.025% nZnO (*7*) β-chitin + 0.01% nZnO.

ratio to 12–18. The swelling ratio of control bandage was slightly increased after 1 week compared to the composite bandages. After 2 weeks, the bandages showed no change in the swelling ratio.

The bandages showed degradation at similar rate with or without nZnO (Fig. 2d). All the bandages degraded about 40–50% after 1 week of immersion in PBS containing lysozyme. The presence of nZnO did not alter rate of degradation of the bandages.

Release Study of nZnO by Inductively Coupled Plasma-Optical Emission Spectrometry (ICP-OES)

The ICP-OES analysis showed that the bandage pieces contained 0.1 (A) and 0.05% (B) of nZnO corresponding to the bandage weight. The release study of nZnO showed that no nZnO was released from the bandage immediately after immersion in PBS. After 1 week, 12% from A and 12.5% of nZnO from B was released.

Haemostatic Potential of β-Chitin Hydrogel/nZnO Composite Bandage

Figure 3a represents the photos of composite bandage, blood on composite bandage and clotted blood on the bandage. The composite bandages showed enhanced blood clotting compared to control and blank (Fig. 3b). The composite bandages caused the activation of platelets thereby causing the blood to clot. Here also the presence of nZnO did not alter the hemostatic nature of β-chitin. The platelets were well activated, attached and spread over the bandage surface (Fig. 3c). It indicates that the bandages were hemostatic in nature.

In Vitro Antibacterial and Antifungal Activity Evaluation

We have evaluated the antibacterial activity of the prepared composite bandages against *S. aureus* (Fig. 4a, b) and *E.coli* (Fig. 5a, b). In the figure, serial dilution of bacteria is indicated from top to bottom and the different samples are indicated from left to right. It was clear from the data that the number of bacterial colonies was decreased in presence

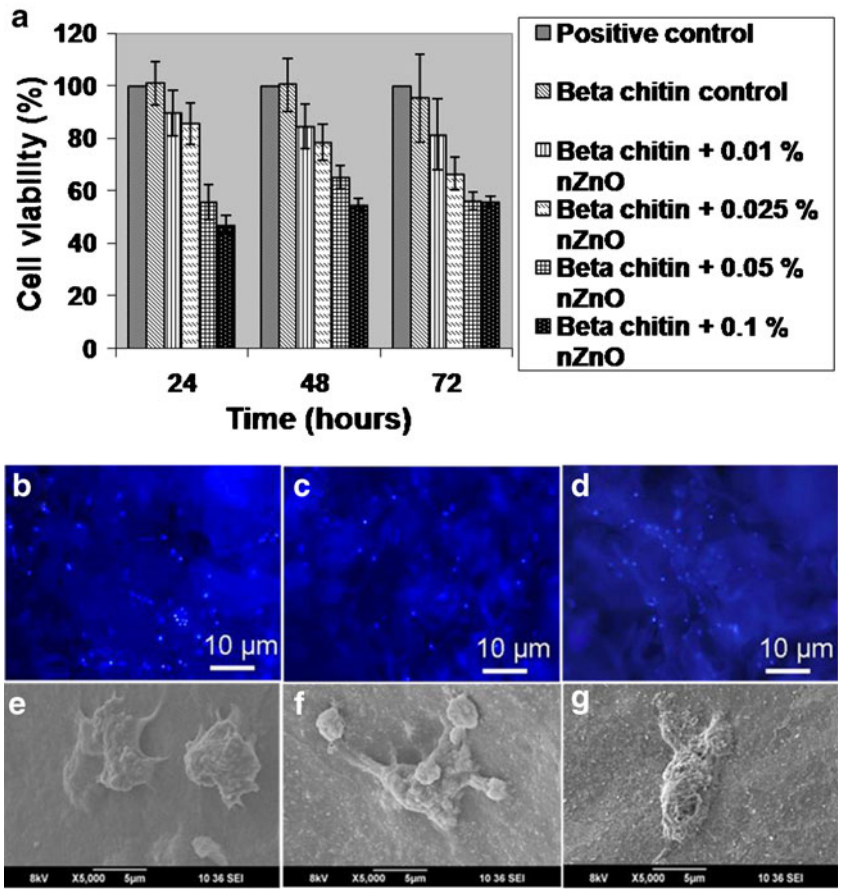

Fig. 6 (**a**) Cell viability study using nHDF cells. DAPI staining of nHDF cells attached on (**b**) β-chitin, (**c**) β-chitin + 0.05% nZnO, (**d**) β-chitin + 0.1% nZnO composite bandages. SEM images of cell attachment on (**e**) β-chitin, (**f**) β-chitin + 0.05% nZnO, (**g**) β-chitin + 0.1% nZnO composite bandages.

of bandages with higher concentrations of nZnO (0.1 and 0.05%). At lower concentrations of nZnO, the antibacterial activity was reduced and this was due to lesser availability of nZnO for interaction with bacteria. The antibacterial activity was same against both *S. aureus* and *E.coli*. The reduction in bacterial colony was due to the interaction of nZnO with the bacteria.

Antifungal activity evaluation was done against *Candida albicans* (Fig. 5c) which proved the toxicity of the prepared composite bandages to fungus. The number of viable fungal colonies were found to be decreased in the presence of bandages with higher concentration of nZnO. The number of colonies increased when the concentration of nZnO was decreased. β-chitin control and Kaltostat did not show any activity against the fungus.

Cell Viability Evaluation

Cell viability of the prepared composite bandages was studied on HDF cells (Fig. 6a). After 24 h of incubation, bandages with higher concentration of nZnO (0.1 and 0.05%) showed 50–60% cell viability whereas bandages with 0.025, 0.01% of nZnO showed 90% viability. The viability remained unchanged after 48 and 72 h. The decrease in the viability was due to the presence of nZnO.

Cell Attachment, DAPI Staining and Phalloidin Staining

DAPI stained images revealed that number of cells were more in control and bandage with lower concentration of nZnO (Fig. 6b, c, d). HDF cell attachment, infiltration and proliferation were assessed by taking the SEM images of bandages with the cells (Fig. 6e, f, g). SEM images showed that there were more number of cells on the surface of control than that on the surface of nZnO containing bandages. Figure 7a–i represents the laser confocal images of bandages; phalloidin stained images and merged images. The data showed that the number of HDF cells attached on the control bandage was more compared to the

Fig. 7 Laser confocal images of the surface of (**a**) β-chitin, (**d**) β-chitin + 0.01% nZnO and (**g**) β-chitin + 0.1% nZnO bandage. Phalloidin dye stained confocal images of the HDF cells attached on (**b**) β-chitin, (**e**) β-chitin + 0.01% nZnO and (**h**) β-chitin + 0.1% nZnO bandage. Merged confocal images of (**c**) β-chitin, (**f**) β-chitin + 0.01% nZnO and (**i**) β-chitin + 0.1% nZnO bandage. Z-stacked laser confocal images of the surface of (**j**) β-chitin, (**m**) β-chitin + 0.01% nZnO and (**p**) β-chitin + 0.1% nZnO bandage. Phalloidin dye stained Z-stacked confocal images of the HDF cells attached on (**k**) β-chitin, (**n**) β-chitin + 0.01% nZnO and (**q**) β-chitin + 0.1% nZnO bandage. Merged Z-stacked confocal images of (**l**) β-chitin, (**o**) β-chitin + 0.01% nZnO and (**r**) β-chitin + 0.1% nZnO bandage (scale represents 200 μm).

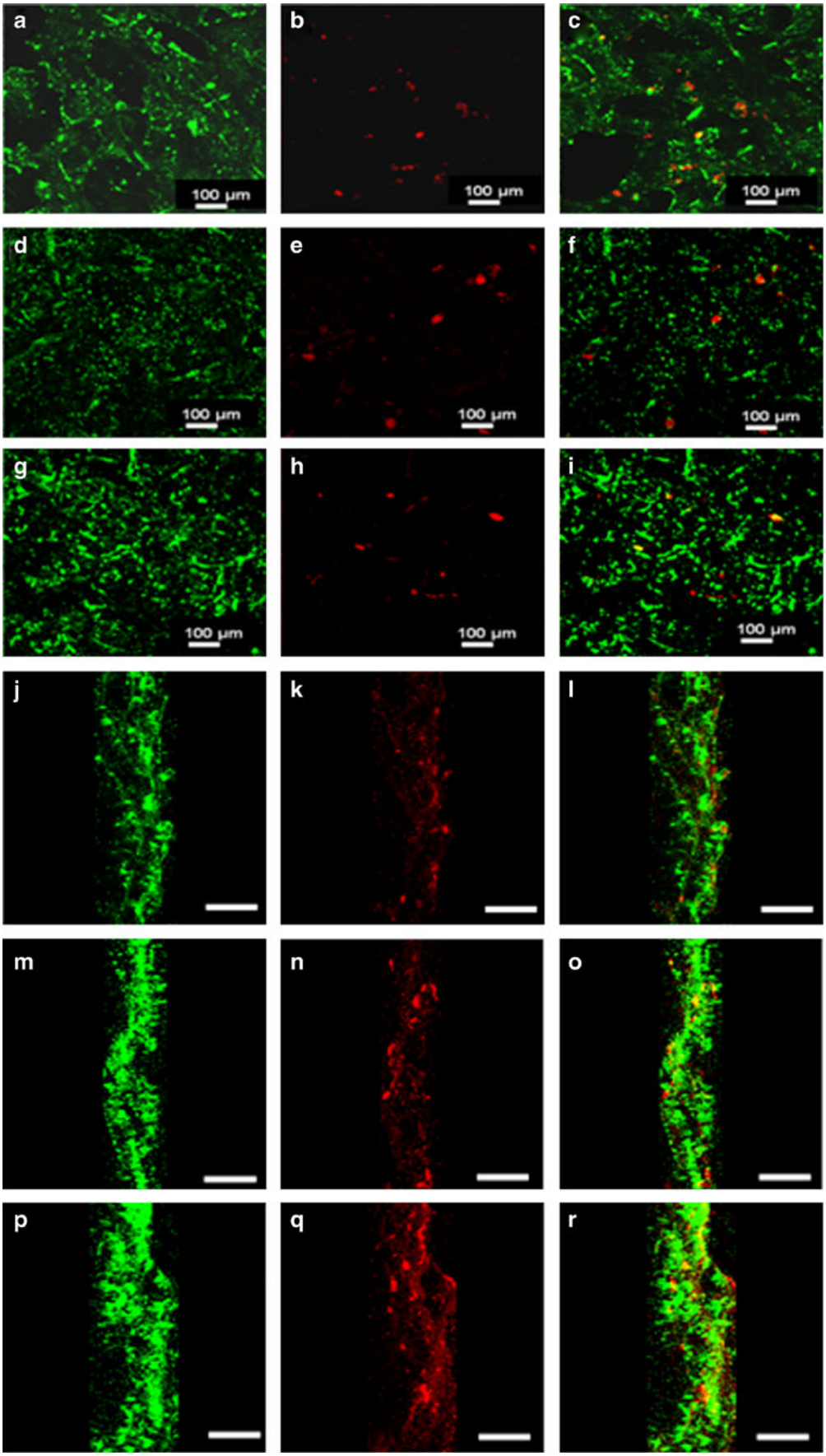
a
100 µm
b
100 µm
c
100 µm
d
100 µm
e
100 µm
f
100 µm
g
100 µm
h
100 µm
i
100 µm
j
k
l
m
n
o
p
q
r

composite bandages. The Z-stacked images (Fig. 7j–r) have proved that the HDF cells infiltrated up to 100 μm after 24 h of incubation.

In Vivo Evaluation

Figure 8a represents the photographs of wound closure and Fig. 8b showed the wound area closure in percentage. It was clear from the data that all wounds healed by 10–20% 1 week after the surgery. Kaltostat™ and bare wound showed 70% of wound closure after 2 weeks whereas wounds treated with β-chitin control and composite bandages showed 85% closure which was significantly high in comparison to the control. After 3 weeks wounds treated with β-chitin control and composite bandages showed 100% closure whereas the wounds treated with Kaltostat™ and bare wound healed showing 90% closure.

Hematoxylin-Eosin Staining (H & E Staining)

Figure 9a represents the H & E stained images of the wound tissues. The images revealed that the granulation tissue was formed on the wounds treated with β-chitin control and composite bandages prominently but the same was very poor in control wound and Kaltostat™ treated wound. The H & E images after 3 weeks of treatment showed the presence of densely packed keratinocytes in the wounds treated with β-chitin control and composite bandages than control wound. Wounds treated with β-chitin control and composite bandages showed complete re-epithelialization and intact epidermis in comparison to the control. Re-epithelialization data (Fig. 9b) indicated that epithelial layer formation was complete in the composite bandage treated wounds compared to the control and bare wound.

Collagen Quantification by Picro-Sirius Red Staining

Figure 10a represents the Picro-Sirius red stained images of wound tissue. From Fig. 10b it was clear that after 1 and 3 weeks of treatment, the collagen deposition was more on wounds treated with β-chitin control and composite bandages than bare wound and Kaltostat™ treated wounds. Collagen quantification was done by histomorphometry. The data showed that after 3 weeks of treatment the collagen deposition was significantly higher in wounds treated with β-chitin

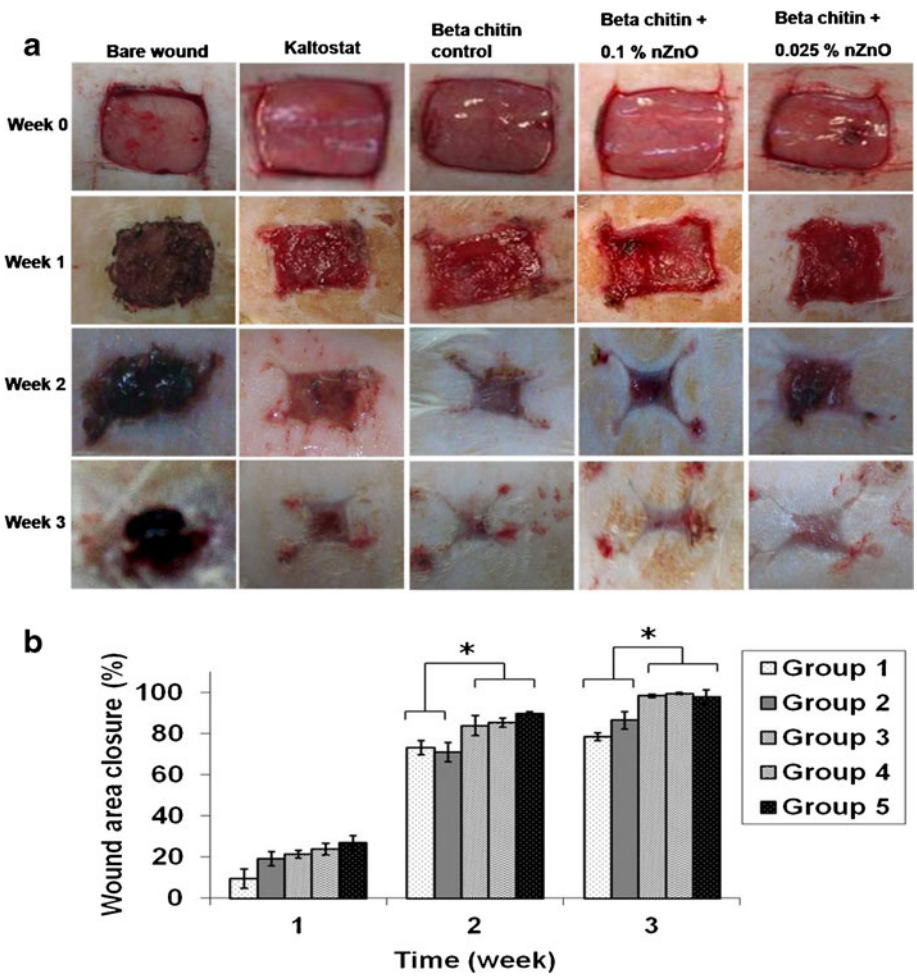

Fig. 8 (**a**) Photographs of bare and wounds treated with composite bandages. (**b**) Wound area closure evaluation data.

control and composite bandages than bare wound and Kaltostat™ treated wounds.

In Vivo Antibacterial Activity Evaluation

Swabs were collected from the rat wounds 1 and 2 weeks after the treatment and were cultured in L.B. broth and plated on L.B. agar plates. The identification of bacterial strains was done using biochemical assays (Table I) and two types of bacteria on the rat wounds were noticed which were *staphylococcus* species and *bacillus* species. The bacteria isolated from the rat wound was quantified and the obtained result indicated a decrease in the number of bacterial colonies by 10,000 and 100,000 times on wounds treated with composite bandage contain 0.025% and 0.1% nZnO after 1 and 2 weeks of the treatment. Both *staphylococcus* and *bacillus* species showed reduction in their growth.

DISCUSSION

The incorporation of nZnO in the composite bandages was confirmed by FT-IR and XRD analysis. The characteristic peaks of XRD and FT-IR were present in the spectra of composite bandages. The intensity of the peaks was higher in XRD spectra of bandages with higher concentration of nZnO compared to the spectra of bandage with lower concentration of nZnO. From this data it was clear that nZnO was incorporated in the composite bandages and the interaction was due to intermolecular hydrogen bonding between the polymer chains of β-chitin and nZnO. Due to the hydrogen bonding, the peak at 3,450 cm^{-1} was (characteristic of hydroxyl group) broadened compared to the β-chitin control. SEM analysis proved the porous nature of the composite bandages. The presence of nZnO did not alter the morphology and porosity of the composite bandage significantly. The interaction between β-chitin and nZnO is due to intermolecular hydrogen bonding. Hydrogen bond is a weak bond compared to ionic and covalent bonds. Hence in this composite bandage, the presence of nZnO did not reduce the porosity significantly. The prepared composite bandages showed interconnected pores with pore size in the range of 200–400 μm. This porous structure would be beneficial not only for the cells to penetrate into the interior and attach on the bandages but also help the transfer of nutrients into the inner parts of the bandage. Apart from that the porous structure

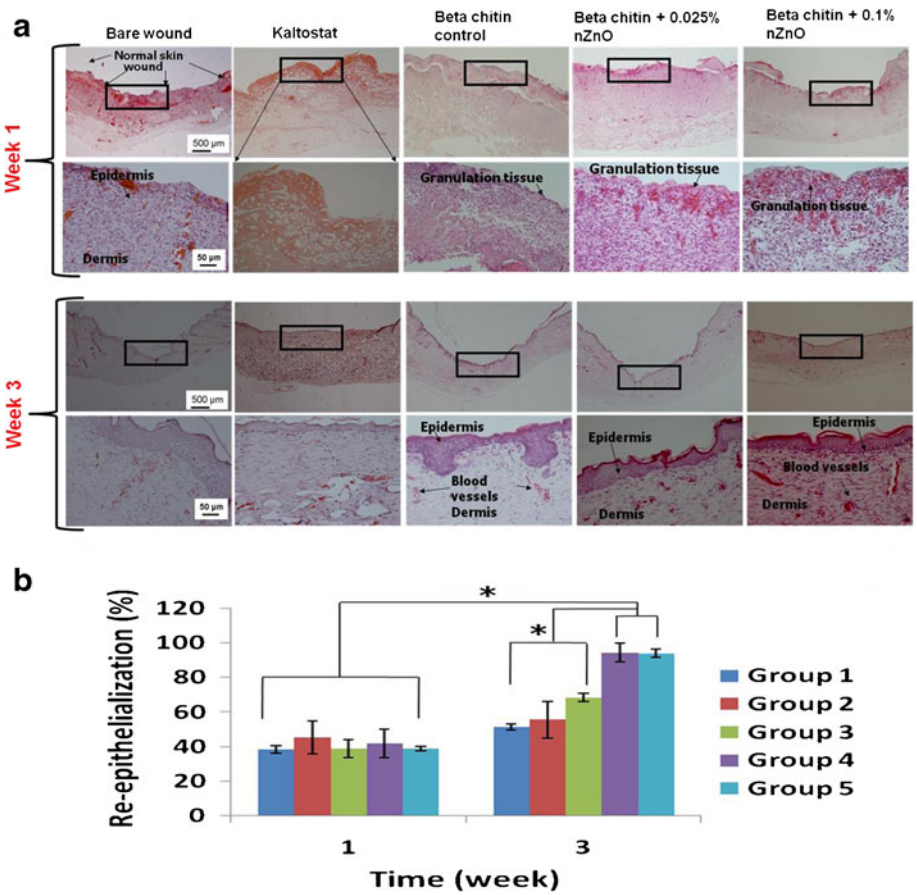

Fig. 9 (**a**) H & E stained images of wound tissue. In week 1 and 3, first row images represents the lower magnification images and second row represents the magnified portion inside the *inset*. (**b**) Re-epithelialization data.

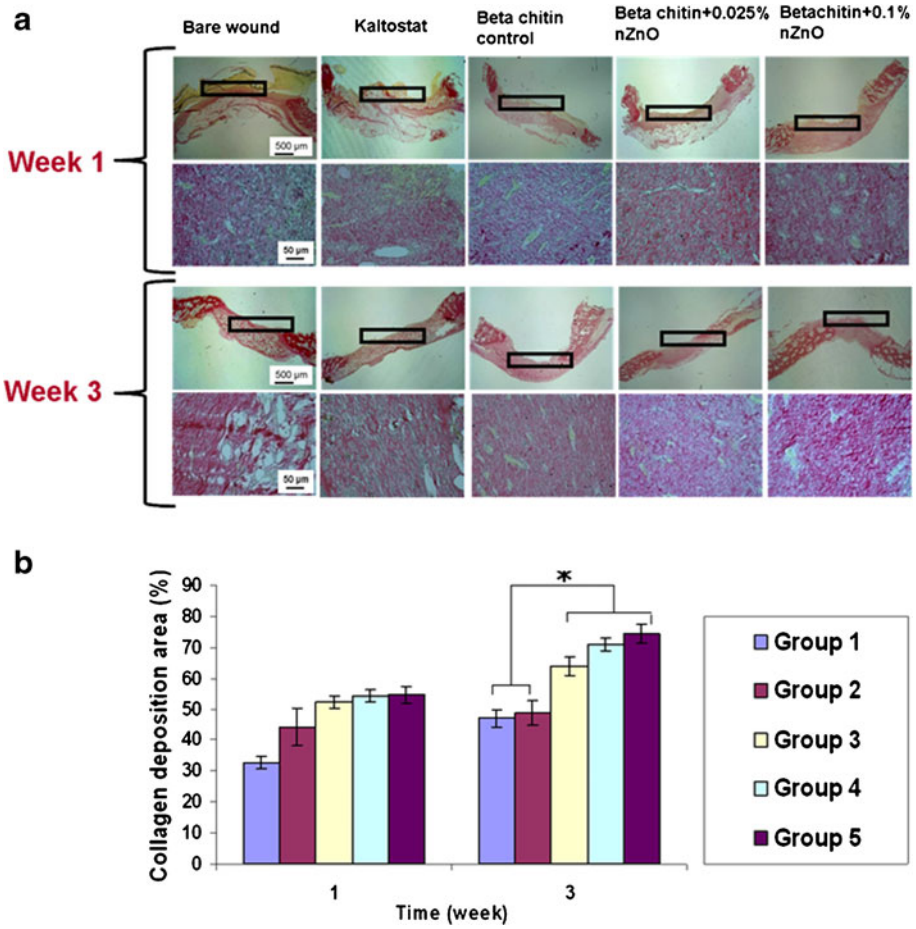

Fig. 10 (**a**) Picro-Sirius red stained images of wound tissue. In week 1 and 3, first row images represents the lower magnification images and second row represents the magnified portion inside the inset. (**b**) Quantification of collagen deposition.

helps to absorb large volume of wound exudate from the wound surface thus can prevent infection.

The composite bandages showed adequate flexibility and tensile strength required for a wound dressing. The bandages did not show any significant difference in the tensile strength compared to the control. Higher concentration of nZnO (0.1%) caused the reduction in the tensile strength however this decrease was insignificant compared to the control bandage. The presence of nZnO caused the reduction of elongation at break compared to the control and this was due to the interaction of nZnO with β-chitin. Even then the bandages showed 40% elongation at break which indicated the flexible nature of the bandage. Due to this flexible nature, these composite bandages can be used for wounds of different shapes. The composite bandages showed high swelling ratio. The presence of nZnO caused a reduction in the swelling ratio. This was due to the interaction of nZnO with β-chitin polymeric chains. The degradation data revealed the degradation nature of composite bandages. All the bandages showed 40% degradation 1 week after the immersion in PBS at 37°C. According to reports, the degradation of β-chitin results in the formation of N-acetyl glucosamine and glucosamine which are biocompatible (13,23). The composite

Table I Identification of Bacteria Isolated by Using Sterile Swab from the Rat Wound Surface by Biochemical Assays

Tests	Staphylococcus species Results	Bacillus species
1. Shape	Round	Rod
2. Gram staining	+ve	−ve
3. Coagulase	+ve	+ve
4. Catalase	+ve	+ve
5. Oxidase	−ve	+ve
6. DNase	+ve	−ve

Table II Quantification of Bacteria Strains Isolated from the Rat Wound by Serial Dilution Method

	Staphylococcus species		Bacillus species	
Sample	Week 1	Week 2	Week 1	Week 2
Bare wound	4×10^{9}	3×10^{8}	6×10^{10}	4×10^{9}
Kaltostat	3×10^{9}	4×10^{8}	8×10^{9}	3×10^{8}
β-Chitin control	9×10^{10}	4×10^{9}	6×10^{10}	3×10^{9}
β-Chitin + 0.025% nZnO	8×10^{6}	4×10^{3}	6×10^{6}	6×10^{4}
β-Chitin + 0.1% nZnO	6×10^{4}	3×10^{2}	4×10^{5}	3×10^{3}

bandages showed similar rate of degradation and the presence of nZnO didn't affect the rate of degradation. Although the presence of nZnO reduced the tensile strength of composite bandage but the decrease was insignificant which was confirmed by student's *T*-test. Due to this insignificant decrease in tensile strength, the degradation profile of composite bandages remains unchanged. The release study of nZnO was analyzed by ICP-OES and the obtained data showed that nZnO was released after immersion in PBS for 1 week. It showed a controlled release after 1 week and reason for slow release might be due to the intermolecular hydrogen bonding between nZnO and β-chitin. The nZnO released from the composite bandage is due to swelling as well as degradation of the bandages when immersed in the corresponding medium. We have done the study up to 1 week since for *in vivo* evaluation the bandages have to be replaced after 1 week.

Hemostatic potential evaluation revealed that the bandages caused faster blood clot formation when blood came in contact with the bandages. The presence of some positive charges on the polymer chains and nZnO caused the blood clot formation. It was confirmed by doing the platelet activation analysis. We analyzed the platelet activation by taking the SEM images and found that more number of platelets were attached and spread throughout the bandage. This data revealed that the bandages were capable of causing the activation of platelets. *In vitro* antibacterial and antifungal activity data of the bandages were promising wherein the bandage with nZnO caused toxicity to gram positive and gram negative bacteria. These composite bandages were toxic to fungus as well. The antibacterial and antifungal activity depends on the concentration of nZnO. In the presence of moisture reactive species from nZnO will be formed and these free radicals can cause the death of bacteria (41). Along with that the electrostatic interaction between nZnO and negatively charged cell wall of bacteria can also cause toxicity to bacteria (39,41). The release of zinc ions from the nZnO can also be the reason for the antibacterial activity (41). The antifungal activity was also due to the production of reactive oxygen species in presence of nZnO and electrostatic interaction between fungus and nZnO (41).

Cell viability studies on HDF cells revealed that bandages with higher concentration of nZnO caused the reduction in cell viability and at lower concentration of nZnO, the viability was increased. It has been reported that nZnO forms reactive oxygen species and zinc ions, which interact with the cells and caused the toxicity (37–39,41). Apart from this the electrostatic interaction between nZnO and cells can also cause toxicity (36,41).

DAPI stained images and SEM images showed that cells were capable of adhering and proliferating on the composite bandages. Cell infiltration was analyzed by taking the laser confocal images of phalloidin dye stained cells attached and infiltrated in the interior and the surface of the bandages.

In vivo evaluation of the prepared bandages were done by applying them on Sprague Dawley rats. The obtained data showed that the wounds treated with the composite bandages healed faster in comparison to the bare and kaltostat treated wounds. Re-epithelialization data showed that wounds treated with the composite bandages and β-chitin control healed faster and the epithelialization was complete within 3 weeks which was significantly higher when compared to the bare and Kaltostat treated wounds. The faster healing and re-epithelialization was due to the migration of more number of fibroblasts and keratinocytes to the wound site. Collagen deposition was analyzed and quantified by picro-sirius red staining and histomorphometry. The wounds treated with composite bandages showed more collagen deposition compared to the control groups. This was due to the influence of β-chitin and nZnO which would have caused the migration of more number of fibroblasts to the wound site and hence caused enhanced collagen deposition. *In vivo* antibacterial activity data revealed that the bandages with nZnO caused a reduction in the growth of bacteria 1–2 weeks after the application of the bandages. The numbers of bacterial colonies were significantly decreased in the wounds treated with nZnO containing bandages whereas the number of colonies was 10,000 times higher in the bare and control wounds (Table II). This reduction in the number of bacterial colonies can be attributed to the presence of nZnO.

CONCLUSIONS

We have developed β-chitin hydrogel/nZnO composite bandage by freeze-dry method. The interconnected micro-porous structure of the bandage enhanced the swelling ratio which would be helpful in absorbing exudates from the wound surface. The composite bandages showed controlled degradation and enhanced hemostatic potential in comparison to the control bandages. *In vitro a*ntibacterial activity and cytocompatibility of the bandages were dependent on the nZnO concentration. *In vivo* evaluation in Sprague Dawley rats showed that the wounds treated with the composite bandages had faster healing, complete re-epithelialization, enhanced collagen deposition and showed reduced number of bacterial colonies compared to the control. The obtained results encourage the use of these bandages for various types of wounds with infection and exudates.

ACKNOWLEDGMENTS AND DISCLOSURES

The authors acknowledge Department of Biotechnology (DBT), India, for the financial support under a grant (BT/PR13885/MED/32/145/2010 dated 03-01-2011). We are also grateful to Nanomission, Department of Science and

Technology, India, which supported this work, under a grant of the Nanoscience and Nanotechnology Initiative program. The author "R. Jayakumar" is grateful to SERC Division, Department of Science and Technology (DST), India, for providing the fund under the scheme of "Fast Track Scheme for Young Investigators" (Ref. No. SR/FT/CS-005/2008). Raja Biswas acknowledges Ramalingaswami Fellowship, Department of Biotechnology, India, for the financial support. P T Sudheesh Kumar acknowledges the Council of Scientific and Industrial Research, India for the Senior Research Fellowship (Award No. 9/963 (0011) 2K11- EMR-1).We are also grateful to Mr. Sajin P. Ravi for his help in SEM analysis. We acknowledge K. S. Sarath for his help in confocal imaging. We are grateful to Dr. P. Reshmi, Dr. A.K.K. Unni, Sajith, Sunil and Sunitha for their help during *in vivo* study. We thank Amrita Centre for Nanosciences and Molecular Medicine for the infrastructure support.

REFERENCES

1. Albertini B, Di Sabatino M, Calonghi N, Rodriguez L, Passerini N. Novel multifunctional platforms for potential treatment of cutaneous wounds: development and *in vitro* characterization. Int J Pharm. 2012. doi:10.1016/j.ijpharm.2012.06.004.
2. Jayakumar R, Prabaharan M, Kumar PTS, Nair SV, Tamura H. Biomaterials based on chitin and chitosan in wound dressing applications. Biotechnol Adv. 2011;29(3):322–37.
3. Kim JO. Development of clindamycin-loaded wound dressing with polyvinyl alcohol and sodium alginate. Biol Pharm Bull. 2008;31 (12):2277–82.
4. Ong SY, Wu J, Moochhala SM, Tan MH, Lu J. Development of a chitosan-based wound dressing with improved haemostatic and antimicrobial properties. Biomaterials. 2008;29(32):4323–32.
5. Willi P, Chandra PS. Chitosan and alginate wound dressings: a short review. Trends Biomater Artif Organs. 2004;18(1):18–23.
6. Balakrishnan B, Mohanty M, Umashankar PR, Jayakrishnan A. Evaluation of an *in situ* forming hydrogel wound dressing based on oxidized alginate and gelatin. Biomaterials. 2005;26(32):6335–42.
7. Berger J, Reist M, Mayer JM, Felt O, Gurny R. Structure and interactions in chitosan hydrogels formed by complexation or aggregation for biomedical applications. Eur J Pharm Biopharm. 2004;57(1):35–52.
8. Howling GI, Dettmar PW, Goddard PA, Hampson FC, Dornish M, Wood EJ. The effect of chitin and chitosan on the proliferation of human skin fibroblasts and keratinocytes *in vitro*. Biomaterials. 2001;22(22):2959–66.
9. Hsieh CY, Tsai SP, Wang DM, Chang YN, Hsieh HJ. Preparation of gamma-PGA/chitosan composite tissue engineering matrices. Biomaterials. 2005;26(28):5617–23.
10. Murakami K, Aoki H, Nakamura S, Nakamura SI, Takikawa M, Hanzawa M, *et al.* Hydrogel blends of chitin/chitosan, fucoidan and alginate as healing-impaired wound dressings. Biomaterials. 2010;31(1):83–90.
11. Kojima K, Okamoto Y, Kojima K, Miyatake K, Fujise H, Shigemasa Y, *et al.* Effects of chitin and chitosan on collagen synthesis in wound healing. J Vet Med Sci. 2010;66(12):1595–8.
12. Patricia MP, Joel G, Jose V, Marjana TC, Irena P, Olivera S, *et al.* Keratin dressings speed epithelialization of deep partial-thickness wounds. Wound Repair Regen. 2012;20(2):236–42.
13. Jayakumar R, Prabaharan M, Nair SV, Tamura H. Novel chitin and chitosan nanofibers in biomedical applications. Biotechnol Adv. 2010;28(1):142–50.
14. Tamura H, Furuike T, Nair SV, Jayakumar R. Biomedical applications of chitin hydrogel membranes and scaffolds. Carbohydr Polym. 2011;84(2):820–4.
15. Madhumathi K, Kumar PTS, Abhilash S, Sreeja V, Tamura H, Manzoor K, *et al.* Development of novel chitin/nanosilver composite scaffolds for wound dressing applications. J Mater Sci Mater Med. 2010;21(2):807–13.
16. Ribeiro MP, Espiga A, Silva D, Baptista P, Henriques J, Ferreira C, *et al.* Development of a new chitosan hydrogel for wound dressing. Wound Repair Regen. 2009;17(6):817–24.
17. Jayakumar R, Chennazhi KP, Sowmya S, Nair SV, Furuike T, Tamura H. Chitin scaffolds in tissue engineering. Int J Mol Sci. 2011;12(3):1876–87.
18. Chandumpai A, Singhpibulporn N, Faroongsarng D, Sornprasit P. Preparation and physico-chemical characterization of chitin and chitosan from the pens of the squid species, loligo lessoniana and loligo formosana. Carbohydr Polym. 2004;58(4):467–74.
19. Mathur NK, Narang CK. Chitin and chitosan, versatile polysaccharides from marines animals. J Chem Educ. 1990;67(11):938–42.
20. Mori T, Okumura M, Matsuura M, Ueno K, Tokura S, Okamoto Y, *et al.* Effects of chitin and its derivatives on the proliferation and cytokine production of fibroblasts *in vitro*. Biomaterials. 1997;18 (13):947–51.
21. Mi FL, Shyu SS, Peng CK, Wu YB, Sung HW, Wang PS, *et al.* Fabrication of chondroitin sulfate-chitosan composite artificial extracellular matrix for stabilization of fibroblast growth factor. J Biomed Mater Res A. 2006;76(1):1–15.
22. Cho YW, Cho YN, Chung SH, Yoo G, Ko SW. Water-soluble chitin as a wound healing accelerator. Biomaterials. 1999;20(22):2139–45.
23. Fan Y, Saito T, Isogai A. Preparation of chitin nanofibers from squid pen beta-chitin by simple mechanical treatment under acid conditions. Biomacromolecules. 2008;9(7):1919–23.
24. Kumar PTS, Abhilash S, Manzoor K, Nair SV, Tamura H, Jayakumar R. Preparation and characterization of novel β-chitin/nano silver composite scaffolds for wound dressing applications. Carbohydr Polym. 2010;80(3):761–7.
25. Gardner KH, Blackwell J. Refinement of structure of beta chitin. Biopolymers. 1975;14(8):1581–95.
26. Ratanajiajaroen P, Ohshima M. Preparation of highly porous β-chitin structure through nonsolvent-solvent exchange-induced phase separation and supercritical CO_2 drying. J Supercrit Fluids. 2012;68(1):31–8.
27. Ratanajiajaroen P, Watthanaphanit A, Tamura H, Tokura S, Rujiravanit R. Release characteristic and stability of curcumin incorporated in β-chitin non-woven fibrous sheet using Tween 20 as an emulsifier. Eur Polym J. 2012;48(3):512–23.
28. Ehrlich H. Chitin and collagen as universal and alternative templates in biomineralization. Int Geol Rev. 2010;52(7):661–9.
29. Ehrlich H. Biological materials of marine origin: invertebrates. The Netherlands: Springer Verlag; 2010. p. 594.
30. Maeda Y, Jayakumar R, Nagahama H, Furuike T, Tamura H. Synthesis, characterization and bioactivity studies of novel beta-chitin scaffold for tissue engineering applications. Int J Biol Macromol. 2008;42(5):463–7.
31. Saito Y, Okano T, Gaill F, Chanzy H, Putaux JL. Structural data on the intra-crystalline swelling of beta-chitin. Int J Biol Macromol. 2000;28(1):81–8.
32. Sharma V, Singh SK, Anderson D, Tobin DJ, Dhwan A. Zinc oxide nanoparticles induce genotoxicity in primary human epidermal keratinocytes. J Nanosci Nanotechnol. 2011;11(5):3782–8.
33. Kocbek P, Teskac K, Kreft ME, Kristl J. Toxicological aspects of long-term treatment of keratinocytes with ZnO and TiO2 nanoparticles. Small. 2010;6(17):1908–17.

34. Ng KW, Khoo SP, Heng BC, *et al.* The role of the tumor suppressor p53 pathway in the cellular DNA damage response to zinc oxide nanoparticles. Biomaterials. 2011;32(32):8218–25.
35. Hackenberg S, Scherzed A, Kessler M, *et al.* Zinc oxide nanoparticles induce photocatalytic cell death in human head and neck squamous cell carcinoma cell lines *in vitro*. Int J Oncol. 2010;37 (6):1583–90.
36. Nair SV, Abhilash S, Divya RVV, Deepthy M, Seema N, Manzoor K, *et al.* Role of size scale of ZnO nanoparticles and microparticles on toxicity toward bacteria and osteoblast cancer cells. J Mater Sci Mater Med. 2009;20(1):235–41.
37. Monteiro RNA, Wiench K, Landsiedel R, Schulte S, Inman AO, Riviere JE. Safety evaluation of sunscreen formulations containing titanium dioxide and zinc oxide nanoparticles in UVB sunburned skin: an *in vitro* and *in vivo* study. Toxicol Sci. 2011;123(1):264–80.
38. Stephan H, Norbert K. Dermal toxicity of ZnO nanoparticles: a worrying feature of sunscreen. Nanomedicine. 2012;7 (4):461–3.
39. Kumar PTS, Lakshmanan VK, Anilkumar TV, Ramya C, Reshmi P, Unnikrishnan AG, *et al.* Flexible and microporous chitosan hydrogel/nano ZnO composite bandages for wound dressing: *in vitro* and *in vivo* evaluation. ACS Appl Mater Interfaces. 2012;4 (5):2618–29.
40. Becheri A, Durr M, Nostro PL, Baglioni P. Synthesis and characterization of zinc oxide nanoparticles: application to textiles as UV-absorbers. J Nanopart Res. 2008;10(4):679–89.
41. Abhilash S, Parwathy C, Deepthy M, Sreerekha PR, Nair SV, Manzoor K. Rapid dissolution of ZnO nanocrystals in acidic cancer microenvironment leading to preferential apoptosis. Nanoscale. 2011;3(9):3657–69.